Features of Mechanical Alloying in Fe–B System

EUGENE P. ELSUKOV, ALEXANDER L. UL'YANOV and GENNADIY A. DOROFEEV

Physical and Technical Institute, Ural Branch of the Russian Academy of Sciences, Ul. Kirova 132, Izhevsk 426001 (Russia)

E-mail: Yelsukov@fnms.fti.udm.ru

(Received June 3, 2003; in revised form August 29, 2003)

Abstract

The sequence and kinetics of solid-phase reactions that take place during mechanical alloying of the mixtures of Fe and B powders with the atomic ratios Fe(68)B(32) and Fe(85)B(15) were investigated by means of Mössbauer spectroscopy and X-ray diffraction. It was established that the initial stage of mechanical alloying includes the formation of nanostructural state in α-Fe particles and the formation of the Fe–B amorphous phase with the atomic fraction of boron up to 20 %. For other conditions being kept constant, a substantial difference in the kinetics of the initial stage in Fe–B and Fe–C systems was discovered. On the basis of indirect experimental data, it is assumed that the kinetics of the stage under consideration is determined by the size of B and C atoms.

INTRODUCTION

A detailed investigation of the initial stages of solid-phase reactions (SPR) during mechanical alloying (MA) allows us to understand their mechanisms at the microscopic (atomic) level. According to one of the generally accepted opinions, the necessary conditions for the realization of the initial stage of heterogeneous SPR are the formation of strongly developed contact surface between the initial components and chemical interaction between the latter. The formation of layered composites with the characteristic size about 1 μm was discovered in Fe–B and Fe–C systems by means of scanning microscopy [1, 2] at the earliest stages of MA. However, the analysis of the first phases formed during MA of iron with *sp* elements (C, Si, Ge, Sn) does not allow one to explain their quantitative yields for the indicated size of the elements of different kinds [3–9]. Because of this, the formation of layered composites in the powder particles is to be considered as a preliminary stage of mechanical mixing which prepares conditions for subsequent mixing at the atomic level. The following microscopic model of the initial stage of MA was proposed [3–9]. With the formation of nanostructures (with grain size $\langle L \rangle$ less than 10 nm), interface regions arise in the α-Fe particles (the nanograin boundary and the distorted near-boundary zones) which are ~1 nm wide. Under the conditions of pulsed mechanical treatment, the atoms of *sp* elements get along the α-Fe grain boundaries, segregate on them and form the first phase there. In particular, for MA in Fe–C system, atomic fraction of C in segregates can be 4–6 % [5, 9], and the first phase to be formed is the amorphous phase Am(Fe–C) with the atomic fraction of C 20 to 25 % [5, 6, 9]. Similarly to carbon, boron forms intercalation phases with metals and has very low solubility in the bcc iron under equilibrium conditions. Because of this, it may be expected that the behaviour of Fe–B system during MA will resemble the behaviour of Fe–C system. Indeed, the formation of the amorphous Am(Fe–B) phase was observed for any concentration of B in the initial mixture [2, 10–14]. It may be concluded on the basis of the published works that the amount of boron bound chemically with iron in the amorphous

TABLE 1
Individual properties of boron and carbon (graphite) [15]

Substance	Density, g/cm^3	Lattice type	Covalent radius, nm	Temperature of melting, K	Enthalpy of evaporation, kJ/mol	Electron configuration
B	2.34	Tetragonal	0.088	2573	539	[He] $2s^2p^1$
C	2.26	Hexagonal	0.077	>4000	711	[He] $2s^2p^2$

phase and in borides after MA is smaller than the corresponding amount for the samples after MA followed by annealing, which can be due to the presence of B segregates in the α-Fe particles. It was assumed in [11] that boron is present only in the disordered interface regions. However, no detailed investigations of the initial stages of SPR under MA in Fe–B system have been carried out until now.

At the same time, investigation of the initial stage of MA in Fe–B system is of interest also from the viewpoint of establishing the differences between the kinetics of the process in this system with that of Fe–C system under the same conditions of mechanical treatment. At the first sight, elemental substances boron and carbon (graphite modification) possess many similar physicochemical properties. They are fragile and belong to high-melting elements. A number of physical characteristics of these materials [15] are listed in Table 1. In fact, the question arises whether the difference in electron configurations of B ($2s^2p^1$) and C ($2s^2p^2$) and, correspondingly, the differences in covalent radii of the atoms of these elements can substantially affect the kinetics of SPR under MA.

In order to study the features of the initial stage of MA in Fe–B system, we chose two compositions of the initial mixture with the atomic ratios Fe(68)B(32) and Fe(85)B(15). The first composition is close to the stoichiometry of Fe_2B boride, corresponds to the compositions of previously investigated mixtures [2, 10–14] containing 20 to 60 % B, and was used to investigate the processes of the formation of amorphous-like structure at the initial stage of MA and the maximal amount of Fe_2B phase at the final stage of MA. The choice of the composition of the initial mixture Fe(85)B(15) was explained by the following considerations. It was demonstrated in [2] that for the 20 % atomic fraction of B MA proceeds in one stage: Fe + B → Am(Fe − B) + Fe. At the same time, this stage of the formation of the amorphous phase is realized under MA of the mixtures with much higher B content (up to 50 %), but in this case it is the initial stage before the formation of borides. The use of Fe(85)B(15) composition allows us to follow the initial stage of MA in detail with the purpose of comparing the kinetics of the SPR with that for the mixture Fe(85)C(15) alloyed mechanically under the same conditions of mechanical treatment as described in [9].

EXPERIMENTAL

A mixture of pure powdered Fe(99.99) and B(99.99) with the atomic ratios of Fe(68)B(32) and Fe(85)B(12) was taken for investigation. Mechanical alloying was carried out in the atmosphere of argon in a ball planetary mill Fritsch P-7 using the milling tools (a vessel with a volume of 45 cm^3 and 20 balls 10 mm in diameter) made of strengthened ball bearing steel ShKh15 (1.0 % C, 1.5 % Cr). Energy intensity of the mill was 2.0 W/g. With the forced air cooled, the vessels and balls were heated during mechanical treatment not higher than to 60 °C. For each MA time, the mass of the loaded powder mixture was 10 g. Possible contamination of the sample with the material of milling bodies was monitored by measuring the mass of the vessel, balls and powder before and after treatment.

Mössbauer studies were carried out with YaGRS-4M spectrometer in the regime of constant accelerations with the source of γ quanta ^{57}Co in Cr matrix with the activity of 50 mCi. The distribution functions for superfine magnetic fields $P(H)$ were obtained

from the spectra using the generalized regular algorithm of solving incorrectly formulated problems [16]. The X-ray structural investigations were carried out with DRON-3 diffractometer with monochromatized CuK_α radiation (with graphite as monochromator). When determining structural parameters, grain size and micro-distortions, the X-ray diffractions were approximated by Foigt functions. Iron powder annealed in vacuum at 850 °C for 2 h was the reference. Thermomagnetic measurements were performed with the set-up of dynamic magnetic susceptibility with the amplitude of alternating magnetic field 1.25 Oe and the frequency of 120 Hz in inert atmosphere (Ar) with the heating rate of 60 deg/min within temperature range 300 to 1100 K.

RESULTS AND DISCUSSION

Fe(68)B(32)

The X-ray diffraction patterns of Fe(68)B(32) after mechanical treatment for different time intervals are shown in Fig. 1. All the X-ray reflections broaden substantially during grinding; the lattice parameter of the bcc phase remains unchanged and corresponds to the lattice parameter of pure α-Fe. For grinding (crushing) time $t_{cr} \geq 4$ h, reflections possibly related to boride Fe_2B appear in the diffraction patterns; the amount of this substance increases with an increase in grinding time. However, even after grinding for 32 h the 100 % boride content cannot be achieved. The absence of reflection near the angle $2\theta \approx 35^\circ$ can be related, similarly to [2], with the formation of metastable form of boride Fe_2B. Broadening of the base of (110) reflection should also be mentioned, which may be due to the contribution from halo of the amorphous-like phase Am(Fe–B).

Additional information was obtained from Mössbauer spectra and the distribution functions of superfine magnetic fields (SFMF) *P(H)* recovered from the spectra (Fig. 2). For $t_{cr} = 2$ h, along with the constituent from α-Fe, a new component with broad distribution of SFMF between 200 and 300 kOe appears, which was correlated in [11–14] with the amorphous-like

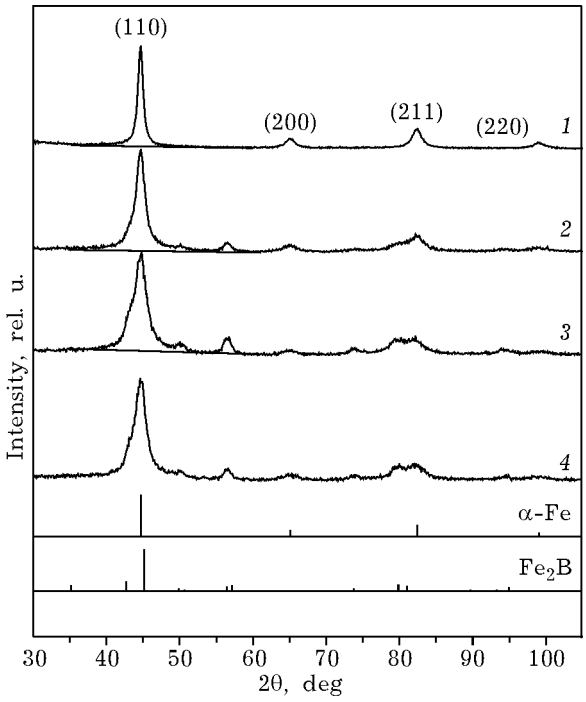

Fig. 1. X-ray diffraction patterns of mechanically alloyed Fe(68)B(32) samples. t_{cr}, h: 2 (*1*), 4 (*2*), 8 (*3*), 32 (*4*).

structure. For $t_{cr} = 4$ h, one more component appears in Mössbauer spectra and in *P(H)* functions; its isomeric shift with respect to α-Fe is $\delta = 0.12$ mm/s, and H = 235 kOe. It relates to the phase which in [12, 17] was called boride $(Fe_2B)'$, because for the equilibrium boride Fe_2B δ = 0.12 mm/s and H = 241 kOe [18, 19]. There are also differences in Curie temperatures of these borides: 955 K for $(Fe_2B)'$ [17] and 1015 K for Fe_2B [18]. We may state on the basis of comparison of the diffraction and Mössbauer results with the data reported in [2, 12, 17] that in all the cases the same stable modification of Fe_2B boride in observed under MA of Fe–B mixtures with the atomic fraction of B about 30 %. In [2], this compound was called x-Fe_2B. In the present work, we will designate this boride, similarly to [12, 17], as $(Fe_2B)'$. With an increase in t_{cr}, the intensity of the component related to the $(Fe_2B)'$ phase increases to ~50 % for t_{cr} = 32 h; that is, MA process is incomplete. It also follows from Mössbauer data (see Fig. 2) that after t_{cr} = 32 h the content of unreacted α-Fe not only did not decrease in comparison with that for t_{cr} = 8 h but even somewhat increased. A likely reason is contamination of the products

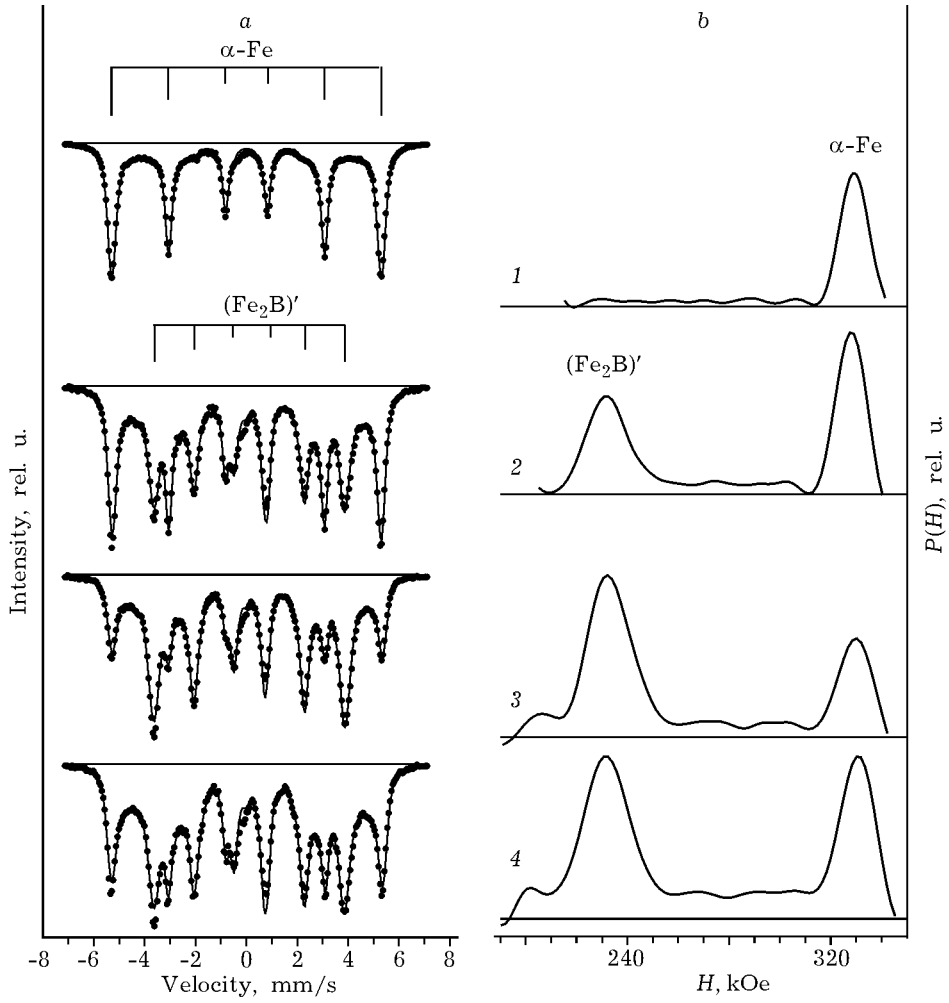

Fig. 2. Mössbauer spectra (*a*) and *P(H)* functions of mechanically alloyed Fe(68)B(32) samples. t_{cr}, h: 2 (*1*), 4 (*2*), 8 (*3*), 32 (*4*).

of solid-phase reactions with the material of grinding bodies (mainly iron) as a result of wear of the vessels and balls of the mill. This contamination becomes noticeable starting from the moment of formation of boride $(Fe_2B)'$, that is, for $t_{cr} \geq 4$ h. In Fig. 3, where the dependencies of an increase in the sample mass and the fraction of pure Fe that did not enter the SPR (the latter value being obtained from the analysis of Mössbauer spectra) on grinding time are shown, one can see that an increase in the sample mass even at $t_{cr} = 8$ h was 4 % mass, further increased at reached 16 % for $t_{cr} = 32$ h. Starting from $t_{cr} = 8$ h, the consumption of Fe for the SPR decreases sharply. The time $t_{cr} = 8$ h is the limiting grinding time for which the contamination of he sample with iron is insignificant (4 % mass). Iron may still exist as a mechanical admixture taking no part in the SPR and therefore having no effect on the reliability of the results obtained.

The results of quantitative analysis of MA of the Fe(68)B(32) mixture are shown in Fig. 4. One can see that the process starts with the formation of the amorphous phase in which the fraction of Fe atoms reaches 20 % for $t_{cr} = 2$ h and remains almost constant during further activation. The $(Fe_2B)'$ boride is the second product of the SPR. The fraction of iron atoms in it increases very rapidly while grinding time increases from 2 to 4 h; by 8 h it reaches the maximal value 53 %. It follows from the data on the evolution of α-Fe grain size (see Fig. 4, *b*) that MA starts in the mixture of Fe and B powders when the system reaches nanostructures state. Minimal achievable grain size is 3 nm. Microdistortions of the bcc lattice

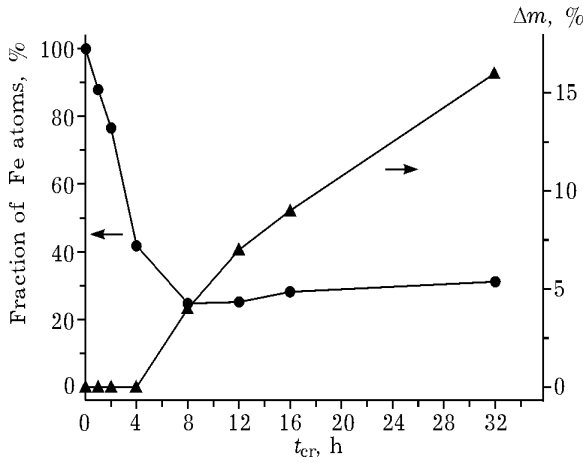

Fig. 3. Atomic fraction of unreacted α-Fe and an increase in the mass of Fe(68)B(32) samples (Δm) *vs.* grinding time t_{cr}.

increase while grinding time increases and reach 0.55 %.

So, the data obtained for MA in the Fe(68)B(32) system completely correspond to those for the SPR as established previously in [2] for the mixtures of a similar composition: Fe + B → Am(Fe − B) + Fe → $(Fe_2B)'$. Nevertheless, because of substantial amount of the wearing products of milling bodies, appearing with the formation of the $(Fe_2B)'$ boride, its 100 % content cannot be achieved during MA.

Fe(85)B(15)

The X-ray diffraction patterns and Mössbauer spectra of mechanically alloyed mixture Fe(85)B(15) are shown in Figs. 5 and 6, respectively. In the diffraction patterns and in the spectra, the main contribution is made by α-Fe for any time of MA. The X-ray reflections broaden, but their positions remain unchanged, that is, no solid solution of boron in α-Fe is formed. For $t_{cr} \geq 4$ h, unusually large width is observed at the base of the bcc reflection (110), resembling a halo of the amorphous phase. This

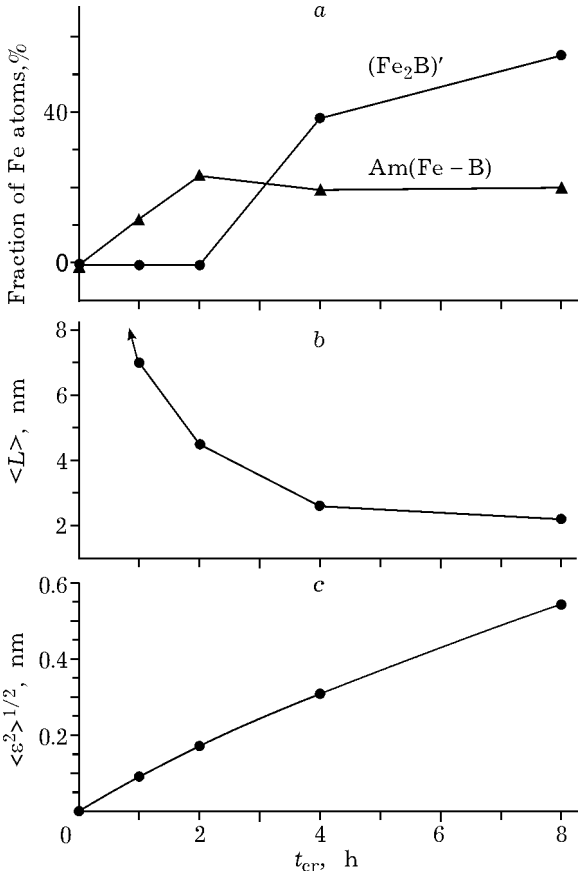

Fig. 4. Atomic fraction of Fe in $(Fe_2B)'$ and in the amorphous phase Am(Fe–B) (*a*), grain size <*L*> (*b*) and microdistortions $<\varepsilon^2>^{1/2}$ in α-Fe particles (*c*) depending on grinding time t_{cr}.

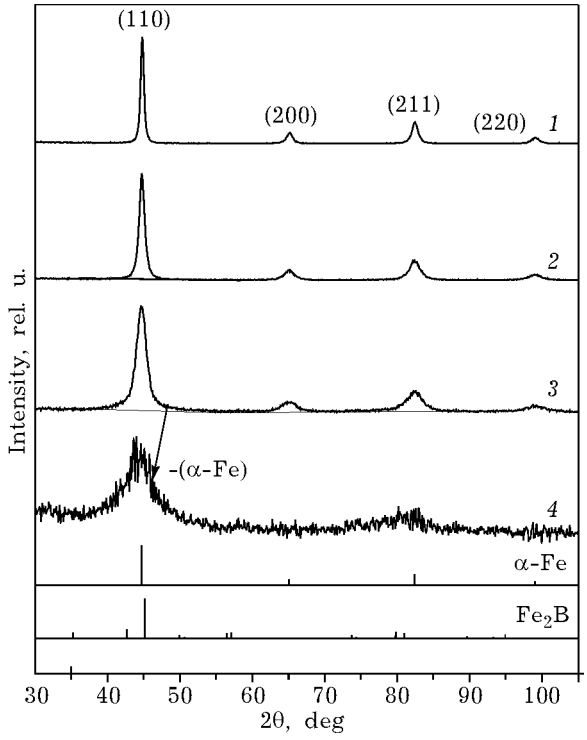

Fig. 5. X-ray diffraction patterns of mechanically alloyed samples Fe(85)B(15). t_{cr}, h: 1 (*1*), 4 (*2*), 16 (*3*); *4* – contribution from the amorphous phase in the diffraction patterns of the sample after MA for 16 h, obtained by subtracting the contribution from the nanocrystalline α-Fe.

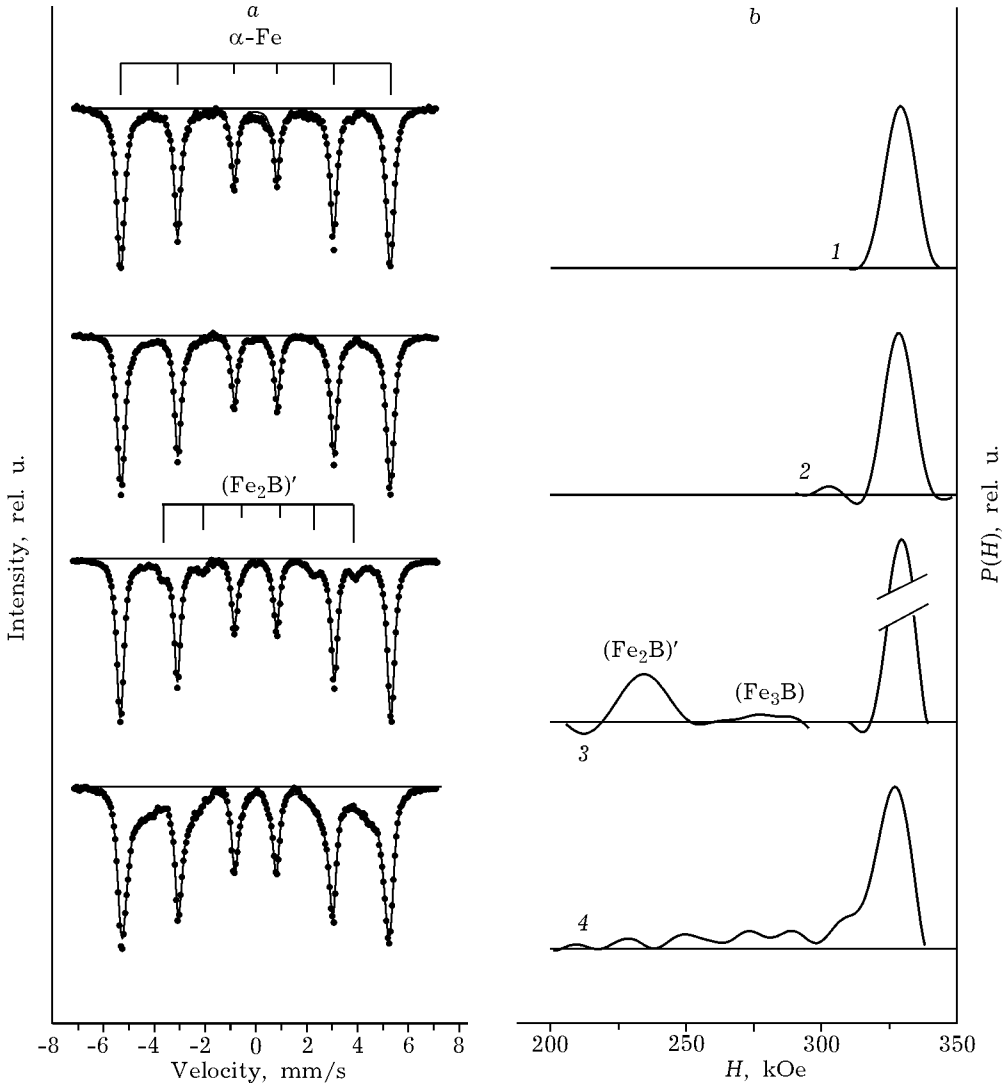

Fig. 6. Mössbauer spectra (*a*) and *P(H)* functions of Fe(85)B(15) samples: *1, 2, 4* – mechanically alloyed, *3* – after MA for 4 h followed by annealing at 400 °C for 1 h; t_{cr}, h: 1 (*1*), 4 (*2*, *3*), 16 (*4*).

broadening is especially noticeable for t_{cr} = 16 h. As a confirmation of the appearance of the amorphous phase Am(Fe–B), the difference curve is shown in Fig. 5; it was obtained by subtracting the lines of *bcc* Fe approximated by Foigt functions from the experimental diffraction patterns of the sample mechanically alloyed for 16 h. This curve consists of two strongly broadened peaks (halo) and resembles the diffraction patterns of the Fe–B amorphous tape [20]. The first weak changes in the Mössbauer spectra of mechanically alloyed samples are observed after t_{cr} = 4 h (see Fig. 6): along with a component from α-Fe, a component with a broad SFMF distribution from 200 to 310 kOe, which should be attributed to the amorphous phase detected in the diffraction patterns. The largest amount of the amorphous phase is formed in the sample after t_{cr} = 16 h.

The fraction of Fe atoms in the amorphous phase, as detected in the Mössbauer spectra, depending on t_{cr} for Fe(85)B(15) (present work) and for Fe(85)C(15) [9] is shown in Fig. 7, *a*. One can see that in the Fe–C system the formation of the amorphous phase starts as early as after t_{cr} = 1 h; during further grinding, its amount increases rapidly and reaches maximum for t_{cr} = 8 h. As we have mentioned above, in the Fe–B system, intensive increase in the amount of the amorphous phase starts only for t_{cr} > 4 h and the maximal fraction of Fe atoms in it at t_{cr} = 16 h is 30 %, which is almost 2 times less

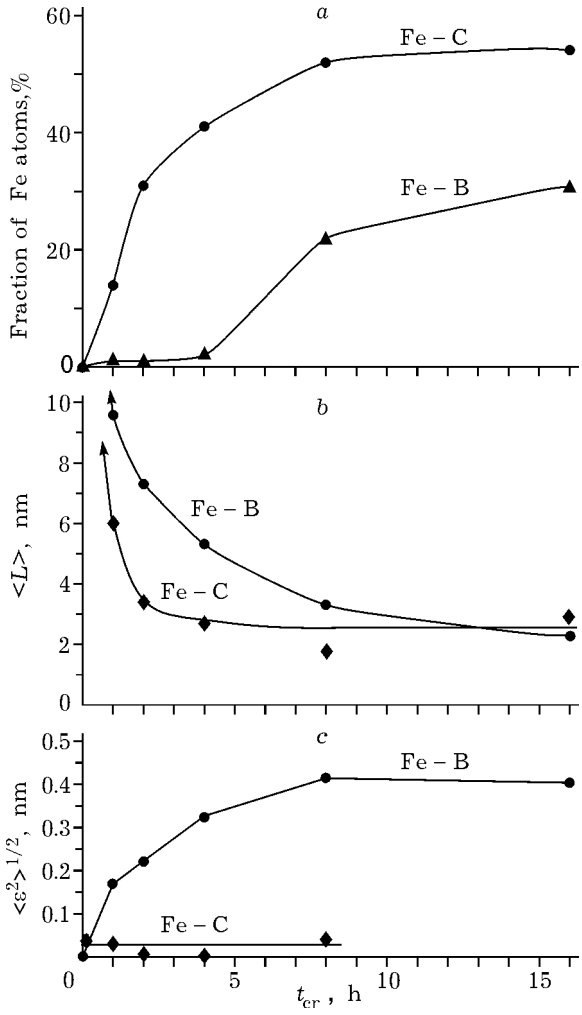

Fig. 7. Comparative quantitative analysis of mechanical alloying in Fe(85)B(15) and Fe(85)C(15) [9] mixtures: *a* – fraction of Fe atoms in the amorphous phase, *b* – size of grains $\langle L \rangle$, *c* – microdistortions $\langle \varepsilon^2 \rangle^{1/2}$ in α-Fe particles.

than that in the Fe–C system. It may be assumed from the comparison between the evolution of the amorphous phase and the changes in α-Fe grain size (see Fig. 7, *b*) that in both systems the condition for the SPR to proceed is the achievement of nanostructured state in α-Fe. It is evident that the nanocrystalline structure is favourable for rapid mass transfer over the grain boundaries: it was demonstrated in [21] that the diffusion coefficient of B in α-Fe at 110 °C is $2.6\,10^{-19}$ m^2/s in the microcrystalline state and $2.6\,10^{-15}$ m^2/s in the nanocrystalline state. As the obtained results indicate, for the identical type of SPR in Fe–B and Fe–C systems, the differences in MA kinetics are manifested not only in the amount of the formed amorphous phase but also in the grain-grinding rate (see Fig. 7, *b*) and in the level of microdistortions (see Fig. 7, *c*).

Let us consider the kinetics of penetration and segregation of B atoms in the boundaries of α-Fe grains. In order to do this, first of all it is necessary to estimate what is the fraction of boron atoms $X^{\mathrm{B}}_{\mathrm{Am}}$, from the initial 15 %, that are chemically bound with Fe atoms in the amorphous phase of the samples after MA. For a known fraction of Fe atoms in the amorphous phase Am(Fe – B) S_{Am} (see Fig. 7, *a*), for determination of $X^{\mathrm{B}}_{\mathrm{Am}}$ it is necessary to have information about the concentration of B in the amorphous phase, which may be determined, in agreement with [19], from mean SFMF values $\bar{H}_{\mathrm{Am}}$ of the amorphous phase for measurement temperature 77 K. Using Mössbauer spectra of mechanically alloyed samples Fe(85)B(15) recorded at the liquid nitrogen temperature, we determined the SFMF distribution functions $P(H)$ and calculated

TABLE 2

Characteristics of phases in Fe(85)B(15) samples after MA followed by annealing

t_{cr}, h	S_{Am}, %	$\bar{H}_{\mathrm{Am}}$ (77 K), kOe	$X^{\mathrm{B}}_{\mathrm{Am}}$, %	$S_{(\mathrm{Fe_2B})'}$, %	$S_{\mathrm{Fe_3B}}$, %	X^{B}_{400}, %
0	0	0	0	0	0	0
1	0	0	0	4.8	0.5	2.5
2	0	0	0	5.1	1.2	3.0
4	2	290	0.5	9.0	2.8	5.0
8	21	287	5	15.0	4.3	9.0
16	30	286	7.5	16.5	8.0	11.0

Note. S_{Am} is atomic fraction of Fe, $\bar{H}_{\mathrm{Am}}$ is mean SFMF, $X^{\mathrm{B}}_{\mathrm{Am}}$ is atomic fraction of chemically combined B in the amorphous phase of samples after MA, $S_{(\mathrm{Fe_2B})'}$, $S_{\mathrm{Fe_3B}}$ are atomic fractions in the phases $(\mathrm{Fe_2B})'$ and $\mathrm{Fe_3B}$, respectively, X^{B}_{400} is atomic fraction of chemically combined B in the phases $(\mathrm{Fe_2B})'$ and $\mathrm{Fe_3B}$ in samples after MA followed by annealing at 400 °C for 1 h.

$\bar{H}_{Am}$ values for the part of $P(H)$ function corresponding to the amorphous phase. The values of $\bar{H}_{Am}$ and S_{Am} for different t_{cr} are listed in Table 2. According to [19], the obtained $\bar{H}_{Am}$ values give an estimation of the maximal atomic fraction of B in the amorphous phase that is 20 %. Therefore, the amount of B chemically combined with Fe atoms in the amorphous phase does not exceed the X^{B}_{Am} values listed in Table 2.

Elucidation of the possibility for boron segregates to be formed at the boundaries of α-Fe grains was carried out similarly to [9] with the help of low-temperature annealing of the samples after MA. First of all, it was discovered that annealing at 400 °C (1 h) of the initial mixture Fe(85)B(15) without grinding did not lead to the formation of any new phases, that is, chemical interaction between Fe and B particles is absent in the mixture at this temperature. Mössbauer spectra of the samples annealed after MA contain a component with $H = 235$ kOe corresponding to boride $(Fe_2B)'$, and a broad component with $H \approx 280$ kOe (see Fig. 6 for the sample with $t_{cr} = 4$ h). The latter may be attributed to metastable boride Fe_3B. The Mössbauer spectrum of this sample consists of three sextets with close SFMF [19, 22]; their weighted average value at room temperature is $\bar{H} = 270$ kOe. In order to carry out additional verification of the formation of Fe_3B boride along with $(Fe_2B)'$ boride, we performed temperature measurements of the dynamic magnetic susceptibility $\chi(T)$; the results are shown in Fig. 8. Here arrows indicate Curie temperature for borides $(Fe_2B)'$, Fe_3B [17, 19] and pure iron α-Fe; temperature of spin re-orientation of borides T_{SRO} is also indicated [18]. The presented results provide evidence that the annealing of mechanically alloyed samples at a temperature of 400 °C (1 h) results in the formation of borides $(Fe_2B)'$, Fe_3B.

By fitting the Mössbauer spectra of the annealed samples with a superposition of three sub-spectra corresponding to the phases α-Fe, $(Fe_2B)'$, Fe_3B, we determined the amount of Fe in the phases $(Fe_2B)'$ ($S_{(Fe2B)'}$) and Fe_3B (S_{Fe_3B}). Total amount of boron atoms X^{B}_{400} (of the initial 15 %) chemically combined in borides was calculated using the stoichiometric relations of these phases. The data on $S_{(Fe_2B)'}$, S_{Fe_3B} and

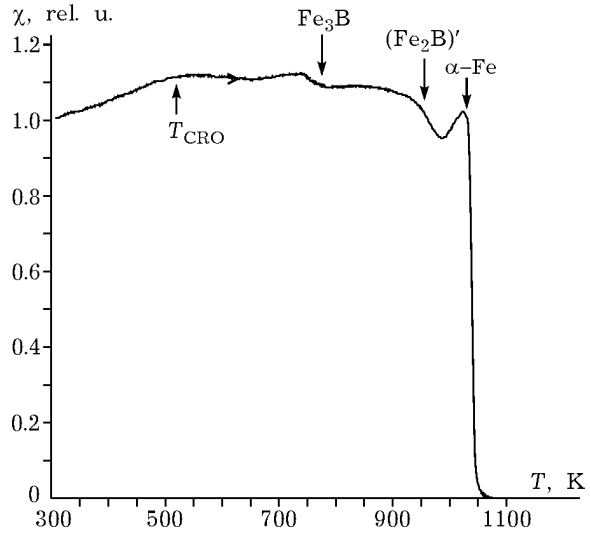

Fig. 8. Temperature dependence of the dynamic magnetic susceptibility of Fe(85)B(15) sample after MA for 16 h followed by annealing at 400 °C for 1 h. For explanations, see text.

X^{B}_{400} are listed in Table 2. Comparison of X^{B}_{Am} and X^{B}_{400} values for mechanically alloyed samples before and after annealing leads to the conclusion that up to 4 % B of the initial 15 % can be present in α-Fe particles in chemically non-combined state. It is logical to assume that B atoms that are not combined chemically exist in the form of segregates on the boundaries of α-Fe grains. In such a model, segregates are a source of B for the formation of the amorphous phase in the interfaces of α-Fe nano-structure during MA. In agreement with Fig. 7, *b*, let us accept the size of non-distorted part of a grain to be $\langle L \rangle = 3$ nm ($t_{cr} = 16$ h), the thickness of boundary in which B is segregated to be 0.3 nm (of the order of one lattice parameter of α-Fe), and the width of the interface (the boundary and the distorted zone near the boundary) which is equal to 1 nm. With these dimensions, the volume fraction of the interface distorted zone will account for 25 %, which is in satisfactory agreement with the value shown in Table 2 $S_{Am} = 30$ % for $t_{cr} = 16$ h.

It also follows from the data obtained that the kinetics of segregate formation under MA in the system Fe(85)B(15) fully coincides with that in the system Fe(85)C(15) [9] both in the time of mechanical treatment and in the atomic fractions of B and C in the segregated state (4 %). Under these conditions, the established

essential difference in the kinetics of the formation of the amorphous phase in Fe(85)B(15) and in Fe(85)C(15) (see Fig. 7, *a*) can be explained by the difference in the covalent radii of B and C atoms and the corresponding different penetration capability of B and C from the segregates into the near-boundary distorted zones. This assumption is indirectly confirmed by comparing the dependences $<L>$ (α-Fe) = $f(t_{cr})$ and $<\varepsilon^2>^{1/2} = f(t_{cr})$ for the systems Fe–B and Fe–C in Fig. 7, *b* and *c*. Intensive penetration of C atoms from the segregates into the near-boundary distorted zone of interfaces does not cause growth of microdistortions but sharply increases the rate of α-Fe grain grinding. The latter was explained in [5] by the fact that a dislocation which comes out on the grain surface and captures into its nucleus a C atom gets anchored and thus acts as a nucleus of a new boundary due to non-anchored dislocations flowing onto it from the grain body. This mechanism also provides relaxation of microdistortions in the interfaces. In the case of MA of Fe and B powders, the behaviour of $<L>$ (t_{cr}) and $<\varepsilon^2>^{1/2}(t_{cr})$ is similar in many aspects to that observed in pure α-Fe during grinding under the same conditions: an increase in $<\varepsilon^2>^{1/2}$ and a slow decrease in $<L>$ are observed with an increase in t_{cr} (for t_{cr} = 16 h, $<L>$ = 9 nm) [23].

CONCLUSION

Mechanical alloying of Fe and B in a ball mill proceeds in two stages: Fe + B → amorphous phase (Fe–B) + Fe → $(Fe_2B)'$ for the mixture Fe(68)B(32), and in one stage Fe + B → amorphous phase (Fe–B) + Fe for the mixture Fe(85)B(15). It was established that the solid-phase reactions proceed under the condition of achievement of nanostructured state in α-Fe particles.

Investigation of the initial stage of MA (formation of the amorphous phase) in the system Fe–B for the mixture Fe(85)B(15) as an example and its comparison with the initial stage in the system Fe–C for Fe(85)C(15) mixture indicated the following essential difference in the kinetics of the solid-phase reactions in these systems.

1. The Fe–B system is characterized by lower rate of formation of the amorphous phase and the rate of grain grinding in α–Fe particles with an increase in the time of mechanical treatment than the rates observed in Fe–C system.

2. The level of microdistortions in the α-Fe particles in Fe–B system at the very beginning of MA reaches 0.2–0.4 %, while in Fe–C system this value does not exceed 0.03 % during the complete MA process.

The differences the kinetics of MA are explained by differences in the covalent radii of B and C within the following model.

1. Formation of interfaces (boundaries and distorted zones near the boundaries) ~1 nm wide in α-Fe particles.

2. Penetration of B and C atoms along the boundaries of α-Fe grains and formation of segregates in them. The above estimations indicate that the kinetics of segregate formation and the amount of B and C in them are similar for Fe–B and Fe–C systems.

3. The formation of the amorphous phase in the distorted zones of interfaces near the boundaries due to intercalation of B and C atoms from the segregates; it is this stage that is assumed to provide differences in the kinetics of MA.

ACKNOWLEDGEMENTS

Authors thank A. V. Zagainov for carrying out the measurements of dynamic magnetic susceptibility.

The work was supported by RFBR (project No. 03–02–32081).

REFERENCES

1 T. Tanaka, S. Nasu, K. N. Ishihara, P. H. Shingu, *J. Less-Comm. Met.*, 171 (1991) 237.
2 H. Okumura, K. N. Ishihara, P. H. Shingu *et al.*, *J. Mater. Sci.*, 27 (1992) 153.
3 E. P. Yelsukov, G. A. Dorofeev, V. A. Barinov *et al.*, *Mater. Sci. Forum*, 269–272 (1998) 151.
4 G. A. Dorofeev, G. N. Konygin, E. P. Yelsukov *et al.*, in M. Miglierini and D. Petridis (Eds.), Mössbauer Spectroscopy in Material Science, Kluwer Academic Publishers, Dordrecht, The Netherlands, 1999, p. 151.
5 E. P. Yelsukov, G. A. Dorofeev, G. N. Konygin *et al.*, *FMM*, 93, 3 (2002) 93.

6 E. P. Yelsukov, G. A. Dorofeev, V. M. Fomin *et al., Ibid.*, 94, 4 (2002) 43.
7 E. P. Yelsukov, G. A. Dorofeev, *Chemistry for Sustainable Development*, 10, 1–2 (2002) 243. URL: http://www-psb.ad-sbras.nsc.ru
8 E. P. Yelsukov, G. A. Dorofeev, A. L. Ul'yanov *et al.*, *FMM*, 95, 2 (2003) 60.
9 E. P. Yelsukov, G. A. Dorofeev, A. V. Zagainov *et al.*, *Mater. Sci. Eng.*, in press.
10 A. Calka, A. P. Radlinski, R. Shanks, *Mater. Sci. Eng.*, A133 (1991) 555.
11 J. Jing, A. Calka, S. J. Campbell, *J. Phys.: Condens. Matter*, 3 (1991) 7413.
12 V. A. Barinov, V. A. Tsurin, E. P. Yelsukov *et al.*, *FMM*, 10 (1992) 148.
13 J. Balogh, T. Kemeny, I. Vincze *et al., J. Appl. Phys.*, 77, 10 (1995) 4997.
14 E. C. Passamani, J. R. B. Tagarro, C. Larica, A. A. R. Fernandes, *J. Phys.: Condens. Matter*, 14 (2002) 1975.
15 J. Emsly, The Elements, Clarendon Press, Oxford, 1989.
16 E. V. Voronina, N. V. Ershov, A. L. Ageev, Yu. A. Babanov, *Phys. Stat. Sol. (B)*, 160 (1990) 625.
17 V. A. Barinov, G. A. Dorofeev, L. V. Ovechkin *et al.*, *FMM*, 1 (1992) 126.
18 K. A. Murphy, N. Herskowitz, *Phys. Rev. B*, 7 (1973) 23.
19 C. L. Chien, D. Musser, E.M. Gyorgy *et al.*, *Ibid.*, 20 (1979) 283.
20 T. Nakajima, I. Nagami, H. Ino, *J. Mater. Sci. Lett.*, 5 (1986) 60.
21 H. J. Hofler, R. S. Averback, H. Gleiter, *Phil. Mag. Lett.*, 68, 2 (1993) 99.
23 E. P. Yelsukov, G. A. Dorofeev, A. L. Ul'yanov *et al.*, *FMM*, 91, 3 (2001) 46.